

High Precision Temperature Control of Normal-conducting RF GUN for a High Duty Cycle Free-Electron Laser

Kai Kruppa¹, Sven Pfeiffer², Gerwald Lichtenberg¹, Frank Brinker², Winfried Decking²,
Klaus Flöttmann², Olaf Krebs², Holger Schlarb² and Siegfried Schreiber²

¹Faculty of Life Sciences, Hamburg University of Applied Sciences, Ulmenliet 20, 21033 Hamburg, Germany

²Deutsches Elektronen Synchrotron DESY, 22607 Hamburg, Germany

Keywords: Nonlinear Systems, Thermal Modelling, Predictive Control, RF Cavities.

Abstract: High precision temperature control of the RF GUN is necessary to optimally accelerate thousands of electrons within the injection part of the European X-ray free-electron laser XFEL and the Free Electron Laser FLASH. A difference of the RF GUN temperature from the reference value of only 0.01 K leads to detuning of the cavity and thus limits the performance of the whole facility. Especially in steady-state operation there are some undesired temperature oscillations when using classical standard control techniques like PID control. That is why a model based approach is applied here to design the RF GUN temperature controller for the free-electron lasers.

A thermal model of the RF GUN and the cooling facility is derived based on heat balances, considering the heat dissipation of the Low-Level RF power. This results in a nonlinear model of the plant. The parameters are identified by fitting the model to data of temperature, pressure and control signal measurements of the FLASH facility, a pilot test facility for the European XFEL. The derived model is used for controller design. A linear model predictive controller was implemented in MATLAB/Simulink and tuned to stabilize the temperature of the RF GUN in steady-state operation. A test of the controller in simulation shows promising results.

1 INTRODUCTION

This paper deals with temperature control of the radio-frequency (RF) GUN for the European X-Ray free-electron laser XFEL at the *Deutsches Elektronen Synchrotron* (DESY). The 1.15 billion Euro XFEL facility with a length of 3.4 kilometers is under construction, (Altarelli et al., 2006). With European XFEL it will be possible to generate intense X-ray laser pulses with a few femtosecond duration. The electrons are accelerated by 101 superconducting modules and forced through an undulator leading to a sinusoidal path and therefore to the release of photons, i.e. synchrotron radiation. This narrow bandwidth photon beam with wavelength down to 0.05 nm allows to take 3D images at the atomic level. Figure 1 shows the XFEL tunnel with accelerator modules.

Simulation methods allow to develop algorithms and model-based feedback schemes even before the European XFEL is in operation. The approaches can be verified and tested by parameters taken from the Free Electron Laser FLASH, which is the first soft

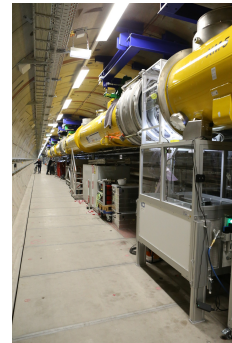


Figure 1: Tunnel of European XFEL (Source: DESY).

X-ray facility ever build and nowadays used for photon science, (FLASH, 2013). Even though FLASH is a smaller facility with a length of 315 meters, it has a comparable structure. The modelling and parameter identification here is done with data from FLASH. With parameter adjustments this model should be used at XFEL, too. This allows to derive control structures for optimal performance of FLASH and the new XFEL even before its operation starts.

The RF GUN is the electron source of the whole facility, (Hoffmann et al., 2015). Temperature control is a very important task in RF GUN operation because a temperature that does not fit the reference value leads to detuning of the cavity. This limits the performance of the RF GUN such that it cannot be operated optimally. A first investigation of a model based controller approach for steady-state operation of the RF GUN as example at FLASH is investigated here. Therefore a thermal model of the RF GUN and its water cooling circuit is derived respecting the influence of the dissipated power of the low-level radio frequency control structures (LLRF). Parameters are identified by fitting the model to measurement data. Moreover simulations of the model can be used internally inside a model predictive controller (MPC) to get optimal signals for RF GUN temperature control. A linear MPC approach shows promising results in simulation.

The paper is organized as follows. In Section 2 the system with cooling circuit and RF GUN with its sensors and actors is described first. Afterwards in Section 3 a dynamical nonlinear model of the plant is developed and the parameters are estimated based on measurement data in Section 4. This model is used to design a model predictive controller in Section 5 which is implemented in MATLAB/Simulink and tested in simulation. Summary and options for future work are given in Section 6.

2 PLANT

This section introduces the main characteristics of the plant that should be modelled. The data and structure of the FLASH facility will be used here to derive the model. The XFEL RF GUN will be similar to FLASH gun such that the basic structure of the model can be applied to XFEL, too. Therefore the setup and the location of important sensors are described. The electron source of the free electron laser is the RF GUN. Electrons are extracted from the cathode and accelerated by an electric field. The microwave power, necessary to accelerate the electrons, is generated by a klystron and is coupled over a waveguide to the gun. The cavity is operated at a resonance frequency of 1.3 GHz. It is very important that the cavity works under tuned conditions at resonance frequency to get an efficient acceleration of the electrons. The gun body is build of copper and has a structure of a hollow cylinder with 1.5 cells. Because of dissipated RF power the RF GUN heats up such that a cooling is necessary to control the temperature of the gun body and to operate the RF GUN under tuned con-

ditions. The average cooling load is in the order of several 10 kW. A schematic cross-section of the RF GUN at FLASH is depicted in Figure 2.

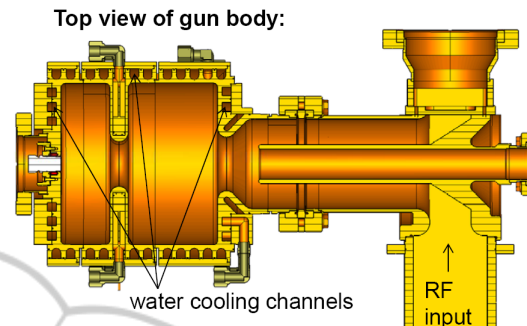


Figure 2: RF GUN at FLASH, (Stephan, 2015).

The system focused here at FLASH consists of the RF GUN controlled by LLRF and the water circuit which supplies the RF GUN with cooling water. Figure 3 shows the schematic setup.

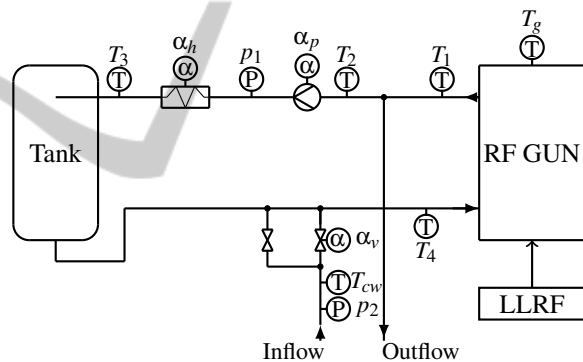


Figure 3: RF GUN with cooling circuit, existing temperature sensors T , pressure sensors p and control inputs α .

The RF GUN is equipped with cooling pipes to control its temperature. They are supplied with cold water. In typical operation ($T_1 > T_4$) warmer water leaves the RF GUN, because the RF GUN heats up due to RF power losses. The water circuit supplying the RF GUN consists of a heater, a water tank, mixing valves and a water inlet and outlet. The mixing valves allow to add cold water of a water reservoir from the inflow to the water circuit to cool the water down. The inflow is controlled by two valves, a small and a big one. Most of the time the big valve is closed such that the whole flow is controlled by the small one. On the other side of the RF GUN water of the same amount is taken out at the water outflow. The volume flow in the circuit is controlled by a pump. If necessary, a heater is available to heat up the water in the circuit. The heater keeps the temperature constant if the

RF GUN is not in operation, such that the water does not cool down to room temperature. A water tank is installed between the heater and the mixing valves. With this tank possible temperature oscillations in the circuit should be damped such that a disturbance in the water temperature is not fed back directly to the RF GUN. The tank acts like a low-pass filter. The cooling water circuit and the RF GUN are provided with several temperature and pressure sensors. All temperature sensors are PT100 sensors with four wire connection. Five temperature sensors T_{cw} and T_1 to T_4 are located in the water circuit outside the RF GUN. The pressure is measured at two locations p_1 and p_2 . The locations of the sensors are depicted in Figure 3. Additionally the control inputs of the pump α_p , the valves α_v and the heater α_h are recorded. Five further sensors measure the temperature inside the RF GUN. The rough position of these sensors in red and the cooling pipes in blue are highlighted in Figure 4.

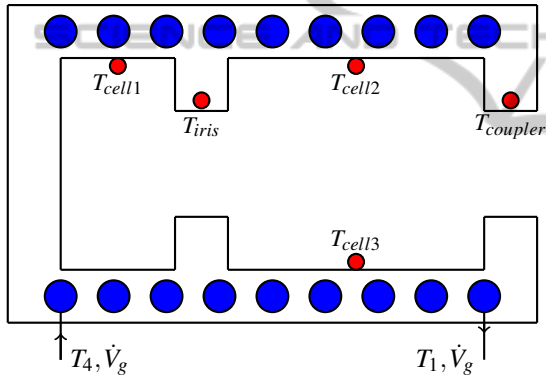


Figure 4: Gun body with sensors.

Three sensors are located near the outside surface of the RF GUN such that they are influenced much by the cooling water. One sensor is at the iris and one sensor at the coupler tube, which is the connection of the RF GUN to the next acceleration modules. The iris sensor T_g is the most representable sensor for the temperature inside the RF GUN.

3 THERMAL MODEL OF THE PLANT

In this section the model of the RF GUN and the cooling circuit is derived. A grey-box modelling approach is used here. Only the effects that influence the dynamics the most should be considered here. All other minor effects are neglected because they have just a small influence on the dynamical behaviour of the component. This leads to models that are not too

complicated and do not need too much computational effort in simulation. This makes them suitable for controller design.

The basis of all following modelling approaches are heat balances. This means that the sum of supplied power $\dot{Q}_{in,i}$ and discharged power $\dot{Q}_{out,j}$ should be equal to the stored power \dot{Q}_{stored} in the component. The supplied power contributes with a positive sign and the discharged power with a negative sign to this balance

$$\dot{Q}_{stored} = \sum_i \dot{Q}_{in,i} - \sum_j \dot{Q}_{out,j}. \quad (1)$$

The heat is given by, (Kuchling, 1991)

$$Q = cpVT, \quad (2)$$

where c is the specific heat capacity, ρ the density, V the volume and T the temperature of the medium.

The thermal behaviour of the RF GUN should be modelled taking into account the influence of LLRF control structures. Operating the RF GUN at a certain acceleration gradient requires RF power controlled by LLRF system. The RF GUN is heated by RF power loss caused by normal conducting resonator. From the RF point of view it is necessary to have a certain gun temperature to operate under tuned conditions. If there are temperature deviations the cavity is detuned. It is still operable but works under suboptimal conditions, e.g. increase in RF power to achieve the nominal accelerating gradient. Therefore the cavity requires additional RF power in this case.

3.1 Cooling Pipes

The RF GUN must be cooled to control its temperature. This is done by cooling pipes that are distributed in the whole RF GUN body. The cooling pipes schematically indicated in blue in Figure 4 are supplied with cold water from the water circuit with temperature T_4 and flow \dot{V}_g . As simplification it is assumed that the water in the pipes is completely mixed with temperature T_r and no flow losses occur. The water leaves the pipes of RF GUN with temperature T_1 and flow \dot{V}_g . Since the pipes cool the RF GUN a heat transfer between cooling pipes and gun body takes place that is proportional to the difference of the temperatures of RF GUN and cooling water with a factor k_{cg} . A small part of the power gets lost to the environment. The environmental temperature is assumed to be constant, because the influence of variations of this temperature on the behaviour of the RF GUN is negligible. It is represented by a constant parameter T_{env} . These losses are modelled by a heat transfer proportional to the difference between the temperatures of the pipe and the environment with constant

of proportionality k_{ce} . The balance of all the powers gives

$$c_w \rho_w V_c \dot{T}_1 = c_w \rho_w \dot{V}_g (T_4 - T_1) - k_{ce} (T_1 - T_{env}) - k_{cg} (T_1 - T_g), \quad (3)$$

where V_c is the volume of the cooling pipes and c_w and ρ_w the specific heat capacity and density of water. Rearranging (3) gives a first order differential equation to compute the return temperature T_1 of the cooling pipes

$$\dot{T}_1 = \frac{\dot{V}_g}{V_c} (T_4 - T_1) - \frac{k_{ce}}{c_w \rho_w V_c} (T_1 - T_{env}) - \frac{k_{cg}}{c_w \rho_w V_c} (T_1 - T_g). \quad (4)$$

3.2 Gun Body

The temperatures of the gun body are measured by five sensors. The temperature distribution inside the RF GUN depends on the electromagnetic field and is very complicated, (Flöttmann et al., 2008). The focus of the model developed here is its applicability for controller design which leads to the negligence of these complex effects.

Because of this the RF GUN is modelled as one body with one temperature T_g representing the thermal behaviour of the whole RF GUN. One of the five sensors should be representable for the RF GUN. The three sensors $T_{cell,i}$, $i = 1, 2, 3$ at the outer surface of the RF GUN are very much influenced by the cooling pipes and do not show the influence of the LLRF properly. The sensor $T_{coupler}$ at the RF GUN exit measures influences from the coupling too. That is why the sensor next to the iris was chosen $T_g = T_{iris}$. It is located next to the middle of the gun body and is influenced by the LLRF as well as by the cooling circuit.

The energy balance of the gun body contains three parts. The heat transfer from the cooling pipes is proportional to the temperature difference of T_g and T_1 with the factor k_{cg} as in (3). The RF GUN has losses to the environment with temperature T_{env} . The heat transfer coefficient is k_{ge} . The third part of the balance is the dissipated power P_{diss} of the LLRF. The powers sum up to

$$c_c \rho_c V_g \dot{T}_g = P_{diss} + k_{cg} (T_1 - T_g) - k_{ge} (T_g - T_{env}), \quad (5)$$

which gives the differential equation of the gun temperature

$$\dot{T}_g = \frac{1}{c_c \rho_c V_g} P_{diss} + \frac{k_{cg}}{c_c \rho_c V_g} (T_1 - T_g) - \frac{k_{ge}}{c_c \rho_c V_g} (T_g - T_{env}). \quad (6)$$

The volume of the RF GUN is denoted by V_g and it is assumed that it is fully build of copper with material constants c_c and ρ_c . The computation of the dissipated power is described in the next part.

3.3 Thermal Influence of the LLRF

The RF GUN is heated by the thermal losses of the LLRF power. The cavity voltage depends on the input power and detuning, i.e. correlated to the RF GUN temperature. If the temperature of the RF GUN deviates from its optimal setpoint, the cavity gets detuned which leads to an increase of reflected power in the cavity and with that the cavity voltage decreases by destructive interference of forward and reflected signal. The following model describes this behaviour of the RF and its thermal effects. The modelling of the RF inside the cavity and its dissipated power are based on (Schilcher, 1998).

If the cavity is supplied by forward power there exists an electric field inside the cavity. Integration of the electric field gives the cavity voltage V_{cav} . The real part of this voltage accelerates the electrons in the cavity. But the RF field also induces a certain surface current at the wall of the cavity which heats up the device. The RF behaviour of the cavity can be modelled by an LCR resonator circuit, shown in Figure 5.

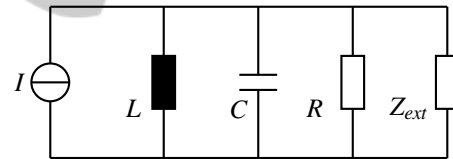


Figure 5: LCR resonator circuit.

The resistance represents the losses that are transferred to the gun body as heat

$$P_{diss} = \frac{|V_{cav}|^2}{R_{sh}}. \quad (7)$$

The shunt resistance R_{sh} is defined as two times the cavity resistance $2R$. The loaded shunt impedance R_L in the LCR circuit is the parallel connection of the cavity resistance and the external load Z_{ext} .

With the electrical equivalent circuit the cavity voltage is given by a second order differential equation

$$\ddot{V}_{cav} + \frac{1}{R_L C} \dot{V}_{cav} + \frac{1}{LC} V_{cav} = \frac{1}{C} \dot{I}, \quad (8)$$

$$\ddot{V}_{cav} + \frac{\omega_0}{Q_L} \dot{V}_{cav} + \omega_0^2 V_{cav} = \frac{\omega_0 R_L}{Q_L} \dot{I}, \quad (9)$$

with the resonance frequency ω_0 and the loaded quality factor Q_L . The circuit is excited by the forward current I coming from the klystron. The stationary

solution of (9) with harmonic excitation $I = \hat{I}_0 \sin(\omega t)$ gives

$$V_{cav} = \hat{V}_{cav} \sin(\omega t + \psi), \quad (10)$$

with the amplitude \hat{V}_{cav} and the angular frequency ω of the cavity voltage and the detuning angle ψ . The angle ψ describes the difference between forward phase and the phase of the cavity voltage

$$\psi = \phi_{for} - \phi_{cav}. \quad (11)$$

Under tuned, which means optimal resonance operating conditions, the phase is equal to the phase of the cavity voltage $\phi_{for} = \phi_{cav}$ such that the detuning ψ is equal to zero. For small frequency deviations $\Delta\omega = \omega_0 - \omega \ll \omega_0$ the detuning and the amplitude variations are given by

$$\tan(\psi) \approx 2Q_L \frac{\Delta\omega}{\omega_0}, \quad (12)$$

$$\hat{V}_{cav} \approx \frac{R_L \hat{I}_0}{\sqrt{1 + \tan^2(\psi)}}. \quad (13)$$

Equation (13) describes the behaviour of the amplitude of the cavity voltage depending on the detuning $\hat{V}_{cav}(\psi)$. Since the forward current is not available as measurement but the forward power P_{for}

$$R_L \hat{I}_0 = R_L \sqrt{\frac{P_{for}}{R_L}} = \sqrt{R_L P_{for}} \quad (14)$$

has to be inserted in (13) to make it usable for a parameter estimation

$$\hat{V}_{cav} \approx \frac{\sqrt{R_L P_{for}}}{\sqrt{1 + \tan^2(\psi)}}. \quad (15)$$

The detuning ψ depends on the temperature of the RF GUN. A change in gun temperature ΔT_g leads to a change in geometry of the RF GUN. The influence of the temperature change on the detuning can be described by a constant factor α such that the temperature change is assumed to be proportional to the tangent of the detuning

$$\tan(\psi) = \alpha \Delta T_g, \quad (16)$$

with proportional constant α . It is assumed that the setpoint $T_{g,SP}$ of the gun temperature is always chosen optimal such that the detuning is zero if T_g is equal to $T_{g,SP}$

$$\Delta T_g = T_g - T_{g,SP} = 0 \Leftrightarrow T_g = T_{g,SP} \rightarrow \psi = 0. \quad (17)$$

Inserting to (16) gives

$$\tan(\psi) = \alpha(T_g - T_{g,SP}). \quad (18)$$

The constant α can be estimated from measurement data by a linear approximation of the relation between

detuning $\tan(\psi)$ and gun temperature. The temperature dependence of the cavity voltage can be computed by inserting (18) into (15) resulting in

$$\hat{V}_{cav}(T_g) = \sqrt{\frac{R_L P_{for}}{1 + \alpha^2 (T_g - T_{g,SP})^2}}. \quad (19)$$

Figure 6 shows the temperature dependence of \hat{V}_{cav} with a chosen value of $\alpha = -26 \frac{1}{K}$. During parameter estimation this turned out to be a typical value for α .

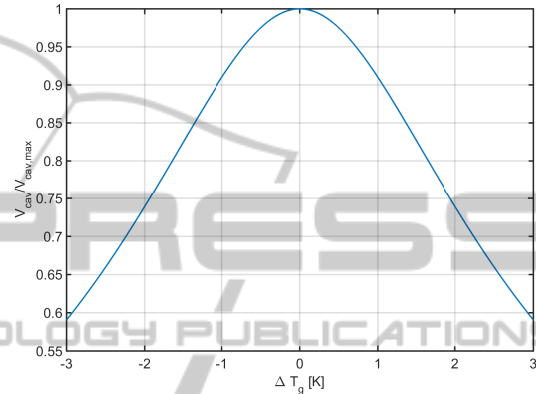


Figure 6: Temperature dependence of the cavity voltage.

3.4 Cooling Circuit

The cooling water circuit supplies the RF GUN with cold water. The model of the circuit is divided into three parts, as depicted in Figure 7. The borders between the different parts are set according to the positions of the temperature sensors T_1, \dots, T_4 .

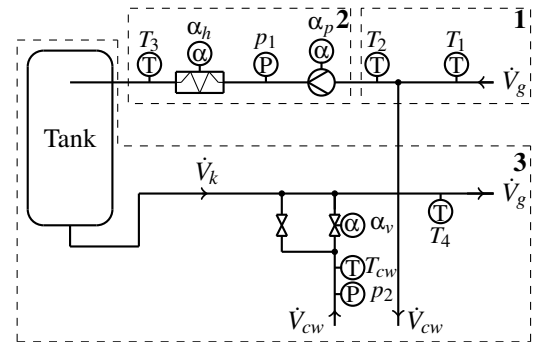


Figure 7: Scheme of the cool water circuit with partitioning for modelling.

The first part of the cooling circuit starts at the water outlet of the cooling pipes of the RF GUN. The water leaves the RF GUN with the flow \hat{V}_g . Its temperature is measured by the sensor T_1 . Since no power is added or removed the temperature T_2 can be modelled by a simple time delay

$$T_2(t) = T_1(t - T_{d,21}). \quad (20)$$

It takes some time since the water from T_1 reaches the second sensor position T_2 . Temperature losses in the pipes are neglected. The flow \dot{V}_g is split up. The flow \dot{V}_{cw} is fed back to the water reservoir. The remaining part

$$\dot{V}_k = \dot{V}_g - \dot{V}_{cw} \quad (21)$$

flows through the water circuit.

In part 2 the temperature is mainly influenced by an electrical heater that heats the water flowing through the device. The added power \dot{Q}_h can be controlled linearly by its control input $\alpha_h \in [0, 1]$ resulting in

$$\dot{Q}_h = \alpha_h \dot{Q}_{h,max}, \quad (22)$$

with $\dot{Q}_{h,max}$ denoting the maximum power of the heater. The heater used here has a specified maximum power of 6 kW. Water with the temperature T_2 enters the heater with a flow \dot{V}_k . Warm water with temperature T_3 leaves the component with the same flow. Building the thermal balance gives

$$c_w \rho_w V_h \dot{T}_3(t) = c_w \rho_w \dot{V}_k ((T_3(t) - T_2(t - T_{d,32})) + \dot{Q}_h(t)), \quad (23)$$

where V_h is the volume of the heater. Rearranging (23) and inserting (22) gives the differential equation for T_3

$$\dot{T}_3(t) = \frac{\dot{V}_k}{V_h} (T_3(t) - T_2(t - T_{d,32})) + \frac{\dot{Q}_{h,max}}{c_w \rho_w V_h} \alpha_h(t). \quad (24)$$

There is a time delay in this part of system, denoted by the parameter $T_{d,32}$.

The water circulates in the pipes because of the pump. It sets up the volume flow \dot{V}_k . The pump is controlled by the signal $\alpha_p \in [0, 1]$. Since no volume flow rate measurements are available in the whole cooling circuit it is hard to model the pump and the volume flow. Thus a linear dependence between the volume flow \dot{V}_k and the control input of the pump is assumed by

$$\dot{V}_k = \alpha_p \dot{V}_{k,max}, \quad (25)$$

with maximal possible flow $\dot{V}_{k,max}$ for $\alpha_p = 1$. The maximal volume flow $\dot{V}_{k,max}$ is a parameter that will be determined during parameter estimation. This simple model can be used because the focus of the overall model is on steady-state operation. Under this condition the volume flow and the control signal just vary a little which justifies a linear approximation of the nonlinear behaviour of the pump around an operating point.

The third part of the cooling circuit contains the most important devices. The water flows through the tank to damp most of the fluctuations in the temperature. Behind the tank, water from a cold water reservoir is added by a mixing valve to cool the water. The measurement information that is available here are the temperatures T_3 and T_4 of the inflowing and outflowing water of the cooling circuit, the temperature T_{cw} of the inflowing cold water, the valve position α_v and the pressure on the reservoir side of the valve.

Since the tank should damp the temperature fluctuations in the circuit a simple model of a low-pass is used here. The output temperature of the tank is unknown. Water with temperature T_3 enters with the flow \dot{V}_k . The unknown output temperature of the tank with volume V_t is denoted by T_x . The thermal balance of the tank gives

$$c_w \rho_w V_t \dot{T}_x = c_w \rho_w \dot{V}_k T_3 - c_w \rho_w \dot{V}_k T_x \quad (26)$$

$$\Leftrightarrow \dot{T}_x = \frac{\dot{V}_k}{V_t} (T_3 - T_x). \quad (27)$$

The water leaving the tank is mixed with the cold water from a reservoir with temperature T_{cw} . The flow \dot{V}_{cw} is not captured by a sensor. Only estimations are possible. The flow is influenced by the valve position α_v . A first modelling approach is a linear dependence of the flow through the valve from the valve position

$$\dot{V}_{cw} = \tilde{\alpha}_v \dot{V}_{cw,max}, \quad (28)$$

with the maximal flow $\dot{V}_{cw,max}$ that should be identified by a parameter estimation. Since the valve does not react instantaneously on a change in the control signal α_v , the reaction of the valve is modeled in Laplace domain (denoted by s) by a linear damping of the control signal resulting in

$$\tilde{\alpha}_v(s) = \frac{1}{T_v s + 1} \alpha_v(s). \quad (29)$$

The mixed flow that supplies the RF GUN is described by

$$\dot{V}_g = \dot{V}_k + \dot{V}_{cw}, \quad (30)$$

$$T_4 = \frac{\dot{V}_k T_x + \dot{V}_{cw} T_{cw}}{\dot{V}_c + \dot{V}_{cw}}. \quad (31)$$

Combining the three parts gives the model of the overall cooling circuit.

3.5 Overall Model

Equations (4), (6), (7) and (19) describing the thermal behaviour of the RF GUN and equations (20) to (31) describing the dynamics of the cooling circuit form

the thermal model of the overall plant. This results in a nonlinear, multiple input, multiple output (MIMO) state space model

$$\dot{\mathbf{x}} = \mathbf{f}(\mathbf{x}, \mathbf{u}), \quad (32)$$

$$\mathbf{y} = \mathbf{g}(\mathbf{x}, \mathbf{u}), \quad (33)$$

with six inputs

$$\mathbf{u} = [T_{g,SP} \ P_{for} \ \alpha_h \ \alpha_v \ T_{cw} \ \alpha_p]^T, \quad (34)$$

five states

$$\mathbf{x} = [T_g \ T_r \ \tilde{\alpha}_v \ T_x \ T_3]^T, \quad (35)$$

and the parameters to be identified

$$\begin{bmatrix} c_w \ \rho_w \ c_c \ \rho_c \ V_c \ V_g \ k_{cg} \ k_{ca} \ k_{ga} \ \alpha \ R_{sh} \ R_L \dots \\ T_{d,21} \ T_{d,32} \ V_h \ V_t \ \dot{V}_{k,max} \ \dot{V}_{cw,max} \ \dot{Q}_{h,max} \ T_{env} \end{bmatrix}^T.$$

The derived MIMO model describes the thermal behaviour of the RF GUN facility taking into account the influence of the water cooling and the LLRF on the gun body. The cross couplings of the cooling and the LLRF power can be simulated by having the control signals of the water circuits α_h , α_v , α_p and the forward power P_{for} of LLRF as inputs to the plant. The whole model was implemented and simulated using MATLAB/Simulink, (Mathworks, 2014b).

4 PARAMETER ESTIMATION

The data available for estimation and validation are recorded with a sampling rate of approximately one second at FLASH. From an LLRF point of view no intrapulse information are used. The model works with average powers. The LLRF signal influencing the gun temperature here is the forward power P_{for} . Its peak values $P_{for,peak}$ are measured by a power meter. The average power follows from

$$P_{for} = P_{for,peak} \tau f_{rep}, \quad (36)$$

with a flattop time τ and a pulse repetition rate f_{rep} of 10 Hz. With this data the parameters of all parts of the model are estimated componentwise first. This means that the parameters of each component on its own are adapted to its input/output measurement data. All parts are fed with measured input data and the parameters are changed such that the quadratic difference between simulated and measured outputs is minimized, (Ljung, 1987). The estimated parameters were cross-validated by a second different data set. The parameter estimations were done by the Simulink Design Optimization Toolbox of MATLAB, (Mathworks, 2014a).

4.1 Componentwise Estimation

The parameters of the RF GUN are identified by feeding the inputs T_4 , \dot{V}_g , $T_{g,SP}$ and P_{for} with measurement data and identify the parameters such that the simulated output signals T_g and T_1 are fit to the corresponding measured values. A simulation of the RF GUN with the resulting parameters and the validation data set shows the results of the parameter estimation of the RF GUN, depicted in Figure 8. Figure 9 shows a zoom in time range of the simulation results. The model captures the dynamics of the RF GUN very well except of a certain offset.

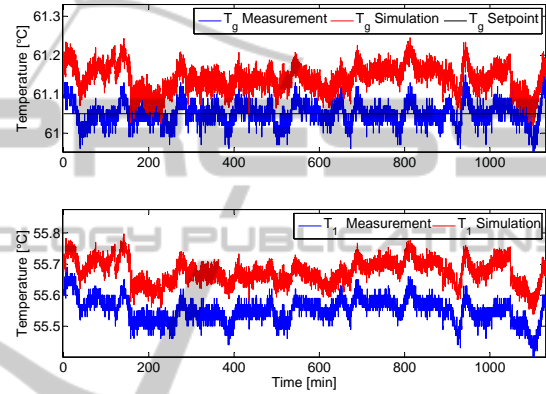


Figure 8: Validation results of the gun model.

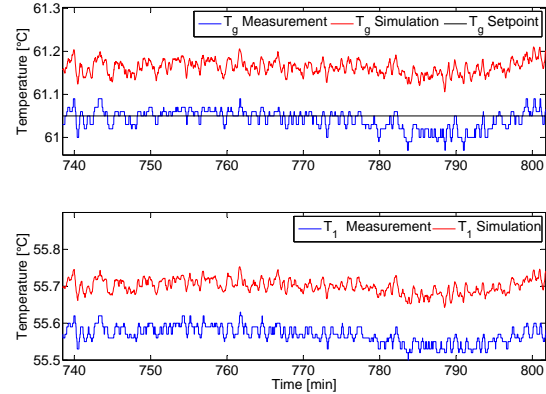


Figure 9: Validation results of the gun model (Zoom).

The parameters of the water circuit were identified with the input signals T_1 , T_{cw} , α_h , α_v and α_p together with the output temperatures T_2 , T_3 and T_4 . The results of the validation simulation are depicted in Figure 10.

The simulation shows that the behaviour at sensor position 2 and 3 are captured well. The model shows the same dynamics. The temperature T_3 only shows an offset. The difference between measurement and simulation of temperature T_4 is much larger.

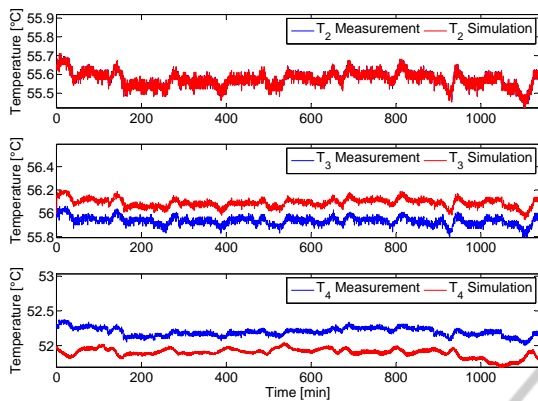


Figure 10: Validation results of the cooling circuit model.

The model does not show all the dynamics of the real system. A reason for this modelling error could be that only few measurement information is available in this part of the system. The behaviour of the tank and the mixing valve are captured together by the sensor T_4 . This makes it hard to model these components, because their effects cannot be measured separately. The missing flow information contributes to the error, too.

4.2 Overall Estimation

After this componentwise estimation of the model parameters, the different parts of the model are linked to the overall model as shown in Section 3.5. This closes the water circuit. The return water of the RF GUN is linked as input to the water circuit which cools the water down and supplies the gun pipes with cold water. With this model a fine tuning of the parameters was done. The results of the simulation with validation data of the RF GUN and the cooling circuit are shown in the following Figures 11 and 12.

These simulations show that the dynamics of the gun temperature in the closed circuit cannot be captured as good as before in the componentwise simulation. These differences can be explained by the modelling errors in the last part of the cooling circuit. The modelling errors occurring in this part are fed back to the RF GUN resulting in a propagation of the error. The simulated gun temperature shows an additional offset, but the main dynamics of the RF GUN are still captured.

The reasons for the modeling errors could be the missing flow information. There are no flow sensors provided even though the flow is a very important item of the model, because it defines the heat power. Flow estimations are very rough. Additionally it is assumed that one temperature sensor represents the whole RF GUN which cannot model the behavior ex-

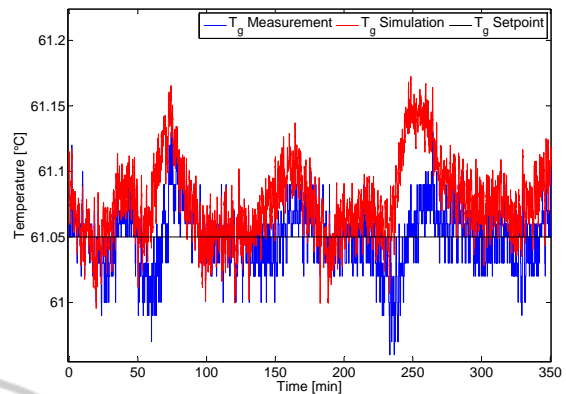


Figure 11: Validation results of the overall model (Gun temperature).

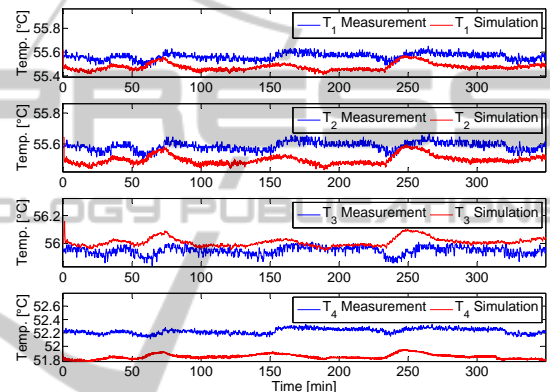


Figure 12: Validation results of the overall model (Circuit temperatures).

actly. But it should be sufficient for controller design.

5 MODEL PREDICTIVE CONTROL

In this part the model of FLASH derived in Section 3 is used to design a model predictive controller (MPC). At each sampling instant the controller computes the optimal future control input with respect to a certain cost function such that e.g. the system follows a given trajectory. A linear MPC approach is used here. This means that first of all the model of Section 3 has to be linearized around a given operating point. After that the linear MPC can be designed and tuned.

5.1 Control Problem

The theory of linear MPC with constraints will now be applied in simulation to control the temperature of the gun, (Maciejowski, 2002). As first controller approach for the facility a controller for a SISO mod-

elled plant is depicted here. The controller should set the position of the valve α_v such that the difference between gun temperature T_g and its set point $T_{g,SP}$ is minimal. The system is disturbed by the cold water with temperature T_{cw} and the environment temperature T_{env} . Figure 13 shows the structure of the design.

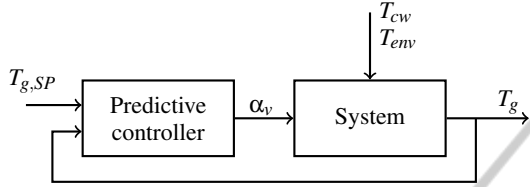


Figure 13: Controller structure.

Inside the controller a linearization of the nonlinear plant model is used to simulate system responses to different input signals. With that an optimal control signal for the plant can be computed. Thus first of all a linear, single input, single output (SISO) model of the nonlinear MIMO model is derived. The controller should stabilize the temperature in steady-state operation. This justifies the use of a linear model. It is valid for a certain range around the operating point. For start up operation of the gun this linear model is probably not suitable. But for steady-state operations it fits the needs. Because of that some inputs of the nonlinear model are set to constants to linearize it

$$T_{g,SP} = \bar{T}_{g,SP}, T_{cw} = \bar{T}_{cw}, \quad (37)$$

$$\alpha_p = \bar{\alpha}_p, \alpha_h = \bar{\alpha}_h \quad (38)$$

The overline indicates the operating point of the corresponding inputs. This does not limit the performance of the model, because the dynamics of the signals does not influence the dynamics of the model extremely. The cold water temperature influences the model, but it is hard to estimate the behaviour of this temperature. As first assumption it is set constant here. The forward power has an enormous influence on the dynamics of the gun temperature. The model in the controller estimates the future states of the gun. Since these states depend on the forward power an estimation of the future forward power has to be found.

Because of that the influence of the LLRF control on the forward power has to be modelled somehow. The LLRF control tries to keep the cavity voltage constant. The cavity voltage decreases if the cavity is detuned. If e.g. the voltage decreases the forward power is increased to compensate the voltage decrease in the cavity. The influence of the detuning on V_{cav} was modelled by (15). With the assumption of a constant cavity voltage a relation between forward

power and detuning can be found resulting in

$$P_{for} = C \frac{1}{1 + \tan^2(\psi)} \quad (39)$$

with an unknown constant factor C .

The dynamic behaviour of the relation should be approximated by a linear model. A black box identification with the System Identification Toolbox gives a first order transfer function model, (Ljung, 2001)

$$G_{LLRF}(s) = \frac{Y_{LLRF}(s)}{U_{LLRF}(s)} = \frac{K_{LLRF}}{T_{LLRF}s + 1} \quad (40)$$

with the input $U_{LLRF}(s) = \alpha(T_g - T_{g,SP})$ and the output $Y_{LLRF}(s) = P_{for}$. The simulation results of the validation of the LLRF model are shown in Figure 14 with $K_{LLRF} = -56$ and $T_{LLRF} = 0.8$.

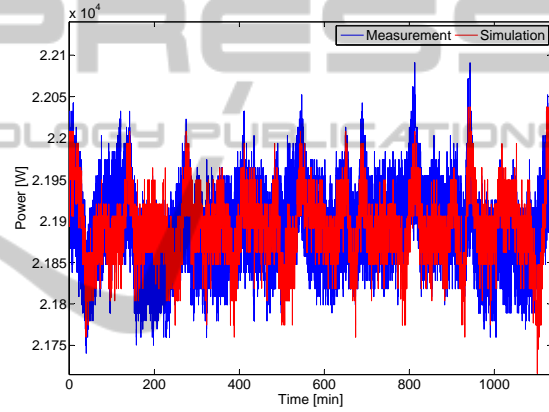


Figure 14: Linear approximation of the forward power P_{for} .

This LLRF model is linked to the plant model of Section 3.5 to generate the forward power P_{for} . Since the first order approximation of the LLRF control is only very rough, this introduces an additional modelling error, but it should be sufficient for the first controller approach here. With the assumptions (37) and (38) this allows us to linearize the nonlinear model around the operation point

$$\bar{\mathbf{x}}_{gun} = [\bar{T}_g \quad \bar{x}_{LLRF} \quad \bar{T}_1 \quad \bar{\alpha}_{v,fil} \quad \bar{T}_x \quad \bar{T}_3]^T, \quad (41)$$

$$\bar{\mathbf{u}} = \bar{\alpha}_v, \quad (42)$$

to get a linear model with 6 states, one input $u_{gun} = \alpha_v$ and one output $y_{gun} = T_g$

$$\mathbf{x}_{gun} = \mathbf{A}_{gun}\mathbf{x}_{gun} + \mathbf{B}_{gun}u_{gun}, \quad (43)$$

$$y_{gun} = \mathbf{C}_{gun}\mathbf{x}_{gun} + \mathbf{D}_{gun}u_{gun}. \quad (44)$$

The state x_{LLRF} is the state introduced by the linear approximation (40) of the behaviour of the LLRF control. The simulation results of the SISO model and its linearization are shown in Figure 15 compared to the

measurement data and the MIMO model. The simulation shows that the approximation of the LLRF control by a linear model (40) adds an offset error. An improvement of the LLRF model could reduce this error. The fast variations of the gun temperature are not captured as good as before as well. Linearizing this model introduces just a small additional error. Because of that it is possible to use the linear model (43) and (44) for control.

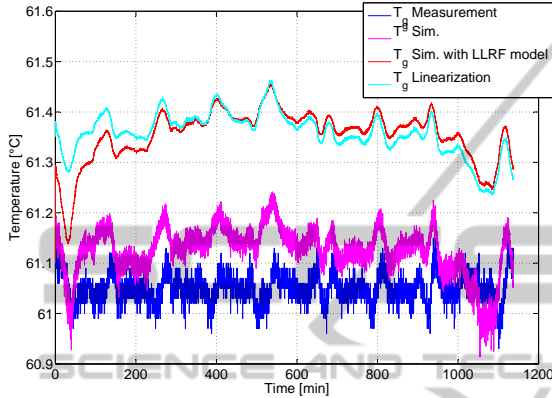


Figure 15: Simulation results of the model without and with LLRF approximation and its linearization.

The theory of MPC is used here according to, (Maciejowski, 2002) meaning that the linear SISO model is used by the MP controller to compute optimal input sequences to the plant according to the cost function

$$J(k) = \sum_{i=1}^{H_p} \|\mathbf{x}_{gun}(k+i) - \mathbf{r}_{gun}(k+i)\|_{\mathbf{Q}(i)} + \sum_{i=1}^{H_u} \|\Delta u_{gun}(k+i)\|_{\mathbf{R}(i)}, \quad (45)$$

where $\Delta u_{gun}(k+i) = u_{gun}(k+i) - u_{gun}(k+i-1)$ are the input changes and $\mathbf{r}_{gun}(k+i) \in \mathbb{R}^{n \times 1}$ the state reference. This means that the states should follow a reference trajectory \mathbf{r}_{gun} with a certain control effort Δu_{gun} . The differences of the states from the reference are weighted by the positive semi-definite matrices $\mathbf{Q}(i) \geq 0 \in \mathbb{R}^{n \times n}$ and the input changes by $\mathbf{R}(i) \geq 0 \in \mathbb{R}^{m \times m}$ at time instance $k+i$. The time range of the prediction is denoted by H_p and of the input changes by H_u . At every time instance the controller solves the optimization problem

$$\min_{u_{gun}(k+i), i=1, \dots, H_u} J(k) \quad (46)$$

subject to $0 \leq u_{gun}(k+i) \leq 1.$

Only the first computed input is given to the plant. The minimization of the cost function is repeated

at every time instance. This is called moving horizon principle. As shown in (Maciejowski, 2002) the optimization problem (46) can be formulated as a quadratic programming (QP) problem with constraints and thus solved very efficiently by standard QP solvers.

5.2 Closed Loop Simulation

In the following the temperature of the RF plant should be controlled by the MPC in a closed loop simulation. The controller gets a reference \mathbf{r}_{gun} for the states. We are only interested in the gun temperature here such that only a reference for this temperature has to be given

$$\mathbf{r}_{gun}(k+i) = \begin{bmatrix} T_{g,SP}(k+i) \\ 0 \\ \vdots \\ 0 \end{bmatrix} \in \mathbb{R}^6, i = 1, \dots, H_p. \quad (47)$$

The tuning parameters are on the one hand the prediction and control horizons H_p and H_u and on the other the weighting matrices \mathbf{Q} and \mathbf{R} . Since only the tracking of the first state, the gun temperature is of interest only this one has to be weighted with a factor q . The factor is chosen the same for all times. This results in a weighting matrix for the states at time i

$$\mathbf{Q}(i) = \begin{bmatrix} q & 0 & \dots & 0 \\ 0 & 0 & \dots & 0 \\ \vdots & \vdots & \ddots & \vdots \\ 0 & 0 & \dots & 0 \end{bmatrix} \in \mathbb{R}^{6 \times 6}, i = 1, \dots, H_p. \quad (48)$$

The weighting of the input changes is done by a scalar since the system has one input only

$$\mathbf{R}(i) = r, i = 1, \dots, H_u. \quad (49)$$

To achieve a good performance of the overall system, the controller can be tuned by changing H_p , H_u , q and r . The parameters H_p and H_u are related to the time that the controller predicts the possible future responses of the plant. The choice of these parameters is a tradeoff between prediction and computation time. The parameters q and r can be tuned to get a tradeoff between tracking and control effort. A higher q leads to better tracking but more control effort in general. The reference temperature $T_{g,SP}$ used here is equal to 61.35°C. This results in a system behaviour shown in Figure 16. Here the difference between setpoint and gun temperature is shown for the simulation of the MPC and measurement data of the device.

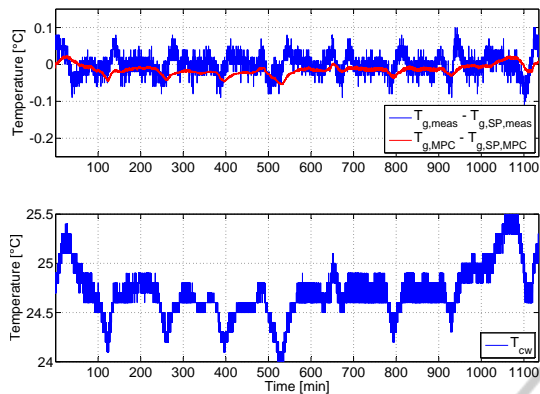


Figure 16: Simulation results of the MPC controller.

In the case where the cold water temperature is constant the controller holds the temperature well except a certain small offset due to model differences. A change in the cold water temperature directly disturbs the gun temperature. The standard MPC approach applied here cannot deal with that, because such disturbance is not predictable. The controller has to be extended with some action for disturbance rejection like integral action.

6 CONCLUSION

A thermal MIMO model of the RF GUN for FLASH was derived. The model focuses on the cooling circuit and the influence of the LLRF to it. Since the structure of the facility at European XFEL is comparable to FLASH the structure of the model can be used and only parameters have to be adjusted. The RF GUN and the cooling circuit are modeled by power balances. With that the main dynamics of the thermal behaviour of the facility are captured. The assumptions that one temperature representing the temperature distribution of the whole RF GUN turned out to be valid. The parameters of the model were estimated by measurement data. Simulation results show good fits of the RF GUN temperature dynamics to the measurement data. In the cooling circuit some differences between simulated and measured temperature occur caused by only few measurement information of the cooling circuit available for parameter identification, especially the missing flow information. With the model a model predictive control approach is derived in simulation to control the gun temperature by the cold water valve. A rough approximation of the LLRF control and a linearization of the model allows the application of a linear MPC approach. Tuning the controller by changing the weights of the cost function and testing it in simulation shows that a predictive

cooling concept can significantly improve the stability of the RF GUN operation compared to the current control concept, i.e. less detuning and therefore less RF power variations leading to constant power dissipation.

In the future the model predictive control concept can be further developed by adding constraints, disturbance rejection or a nonlinear approach. An improvement of the model would be possible with better measurement information e.g. by a mobile flow measurement. Afterwards the controller could be realized on hardware at XFEL and test can be conducted at FLASH. Additionally the model could be used for other approaches like model-based fault detection. This makes sense because of the high complexity of the whole free-electron laser facility.

REFERENCES

- Altarelli, M., Brinkmann, R., Chergui, M., Decking, W., Dobson, B., Düsterer, S., Grübel, G., Graeff, W., Graafsma, H., Hajdu, J., Marangos, J., Pflüger, J., Redlin, H., Riley, D., Robinson, I., Rossbach, J., Schwarz, A., Tiedtke, K., Tschentscher, T., Vartanants, I., Wabnitz, H., Weise, H., Wichmann, R., Witte, K., Wolf, A., Wulff, M., and Yurkov, M. (2006). *XFEL, the European X-ray free-electron laser: Technical design report*. DESY XFEL Project Group, Hamburg.
- FLASH (2013). Free-electron laser FLASH.
- Flöttmann, K., Paramonov, V., Skasyrskaya, A., and Stephan, F. (2008). Rf gun cavities cooling regime study. Desy report, TESLA-FEL 2008-02.
- Hoffmann, M., Ayzvayan, V., Branlard, J., Butkowski, L., Grecki, M. K., Mavric, U., Omet, M., Pfeiffer, S., Schlarb, H., Schmidt, C., Piotrowski, A., Fornal, W., and Rybaniec, R. (2015). Operation of normal conducting rf guns with mtca.4. In *IPAC - 6th International Particle Accelerator Conference, Richmond, USA*. DESY Hamburg, FastLogic Sp. z o.o., Lodz, Warsaw University of Technology.
- Kuchling, H. (1991). *Taschenbuch der Physik*. Fachbuchverlag Leipzig, 13. edition.
- Ljung, L. (1987). *System identification: Theory for the User*. Englewood Cleffs, Prentice-Hall.
- Ljung, L. (2001). *System Identification Toolbox*. The Math Works.
- Maciejowski, J. (2002). *Predictive Control with Constraints*. Pearson Education Limited.
- Mathworks, I. (2014a). *Simulink Design Optimization User's Guide*. The Mathworks Inc.
- Mathworks, I. (2014b). *Simulink User's Guide*. The Mathworks Inc.
- Schilcher, T. (1998). *Vector Sum Control of Pulsed Accelerating Fields in Lorentz Force Detuned Superconducting Cavities*. PhD thesis, Hamburg University.
- Stephan, F. (2015). private communication. DESY.